C h a p t e r 4

EQUATION OF STATE AND PRESSURE-INDUCED CAVITATION OF A CU-ZR BINARY MODEL METALLIC GLASS AND LIQUID

We determined the isothermal equation of state (EOS) in a wide range of temperatures and pressures by carrying out molecular dynamics simulations on a simple binary model metallic glass. A universal form of EOS proposed by Vinet et al. is utilized to fit the data, assuming no phase transitions. Pressure-induced cavitation was observed in glassy states and liquids from our simulations. The thermodynamic limit of instability and kinetic limit of instability of the cavitation behavior were analyzed. Negative pressure is critical to trigger the cavitation. The cavitation barrier height was estimated from the classical nucleation theory. The intrinsic origin of cavitation and its connection to Poisson's ratio or the ratio of G/B are investigated. The relationship to the deformation and fracture behavior of glasses is discussed.

4.1. Introduction

It is of primary importance in both the basic and applied sciences of fluids or solids to obtain the equation of state (the pressure, volume, temperature (P-V-T) relation). This

determines the values of fundamental thermodynamic parameters and helps the general understanding of the behavior and applications of a condensed matter. As a fairly new class of materials, metallic glasses have acquired considerable attention from scientific and technological viewpoints in the last two decades [1, 2]. Unfortunately, to date, knowledge of the isothermal equation of state (EOS) of metallic glasses is still far from complete. Wang and co-workers studied the elastic properties, as well as the pressure dependence of Zr- and Pd-based bulk metallic glasses at ambient temperature in a limited pressure range (up to several GPa) and obtained the EOS in terms of the Murnaghan form [3-5]. In this chapter, we present the isothermal EOS in a wide range of temperatures and pressures by carrying out molecular dynamics (MD) simulations on a simple binary model metallic glass. A universal form of EOS proposed by Vinet et al. [6] is utilized to fit the data, assuming no phase transitions.

To describe the yielding in metallic glasses, a Cooperative Shear Model has been developed for the glassy state based on Potential Energy Landscape (PEL) / Inherent State (IS) theory [7-9]. A scaling relationship among the shear flow barrier, a universal critical yield strain, and the isoconfigurational shear modulus G was constructed [9]. The model reveals that for a fixed glass configuration, the barrier height for shear flow is proportional to the isoconfigurational shear modulus G. It is also found that G has a strong dependence on the specific configurational potential energy of the equilibrium liquid, and the temperature dependence of G in the liquid state is directly related to the fragility of the metallic-glass-forming liquid [10, 11]. In addition, based on the link between elastic softening and configurational changes, a rheology law of metallic-glass-forming liquids has

been proposed and validated, in which G was identified as the effective thermodynamic state variable controlling flow [12]. The isoconfigurational shear modulus G plays a controling role in understanding the yielding and rheological behavior of metallic glasses and liquids, and it can be utilized to design and develop rather fragile glass-forming systems with high ductility and toughness [13-15]. It is therefore natural to ask how the bulk modulus B is related to the yielding and fracture behavior of metallic glasses. Zhang and co-workers reported the different deformation and fracture behavior in metallic glass under compressive vs. tensile loading [16]. It was proposed that the compressive fracture of metallic glass is mainly controlled by the shear stress, while the tensile fracture originates from radiate cores induced by normal stress, and then propagates mainly driven by shear stress. Another intriguing observation is void formation inside shear bands during deformation in metallic glass [17]. It is widely believed that cavitation is closely related to the fracture behavior of metallic glass. However, how and at what stage in deformation a cavity forms remains unclear.

Here, pressure-induced cavitation is observed in glassy states and liquids from MD simulations. The thermodynamic limit of stability and kinetic limit of stability of the cavitation behavior are analyzed and interpreted using the isothermal EOS. Negative pressure is critical to trigger the cavitation. In the simulations, when the negative pressure approaches half the value of the spinodal pressure, the cavitation is triggered. Based on the results, we examine the role of the elastic constants, G and B, the ratio G/B, and Poisson's ratio on the deformation and fracture behavior of the liquid and glassy states.

4.2. MD Simulations

In order to obtain numerical results for the isothermal EOS, we performed MD simulations using an interatomic many-body Rosato-Guillope-Legrand (RGL)-type potential model developed for the Cu-Zr binary alloy system [11, 18]. The original simulation cell contains N = 2000 atoms, arranged in a random bcc structure with periodic boundary conditions. At the beginning, the system was heated to 2400 K and the structure of the liquid phase was allowed to equilibrate (constant-temperature, constant-thermodynamic-tension (TtN) method). The system was then cooled to 50 K under zero pressure using a quenching rate of 2.5 K/ps (1 ps = 10^{-12} seconds) to generate the glass configuration. The glass transition occurs at 700 K. This yielded the reference shapes and size matrices, h_0, in the Parrinello-Rahman formalism. Starting with the cell volume V set at the equilibrium value V_0 (corresponding to zero pressure) at each temperature, we carried out constant-temperature and constant-volume (NVT) simulations at incrementally larger and smaller volume values to obtain the isothermal EOS. Upon determining the P-V relation, NVT simulations were then carried out by first equilibrating 10,000 steps and then followed by another 100,000 steps for each state point, where a time step is set to 1 fs (1 fs = 10^{-15} seconds). The equilibration at each state point was monitored by the total energy and pressure of the simulation cell.

4.3. Results and Discussions

Figure 4.1 shows the pressure change with atomic volume of the $Cu_{46}Zr_{54}$ binary model metallic glass and liquid at different temperatures ranging from 300 K to 1500 K. The data points in Fig. 4.1 were directly obtained from MD simulations, and the pressure is from ~ +6 GPa to ~ -6 GPa. Vinet, Smith, Ferrante, and Rose proposed a universal EOS for all classes of solids in the absence of phase transitions, and its applicability was examined by comparing the predictions from the universal EOS with experimental data for different typical materials [6]. Here, we utilized the Vinet-Smith-Ferrante-Rose universal EOS to fit the MD simulation data of the Cu-Zr binary model glass, and excellent fitting results were found. As shown in Fig.4.1, the solid curves represent the fits. The universal EOS has the following form:

$$P(T,X) = \frac{3B_0(T)}{X^2}(1-X)\exp[\eta_0(T)(1-X)], \tag{4.1}$$

where

$$X \equiv [\frac{V}{V_0(T)}]^{1/3}, \tag{4.2}$$

and

$$\eta_0(T) = \frac{3}{2}\{[\frac{\partial B}{\partial P}]_0(T) - 1\}. \tag{4.3}$$

A knowledge of three equilibrium quantities at each fixed temperature T is necessary for the fitting: the equilibrium volume V_0, isothermal bulk modulus B_0, and isothermal $(\frac{\partial B}{\partial P})_0$.

The notation $(\frac{\partial B}{\partial P})_0$ denotes the zero-pressure value of the isothermal pressure derivative of the isothermal bulk modulus, $(\frac{\partial B}{\partial P})_{T,P=0}$. Based on the fitting parameters, plots of volume vs. temperature and bulk modulus vs. temperature were drawn and compared with previous MD simulation results. The equilibrium bulk modulus Debye-Grüneisen slope from the fitting results was calculated to be [dB/dT] = -35 MPa/K and an exceptional consistency is found [11]. It is obvious that the isothermal EOS can be employed to analyze the pressure dependence of the glass-transition temperature for this model metallic glass.

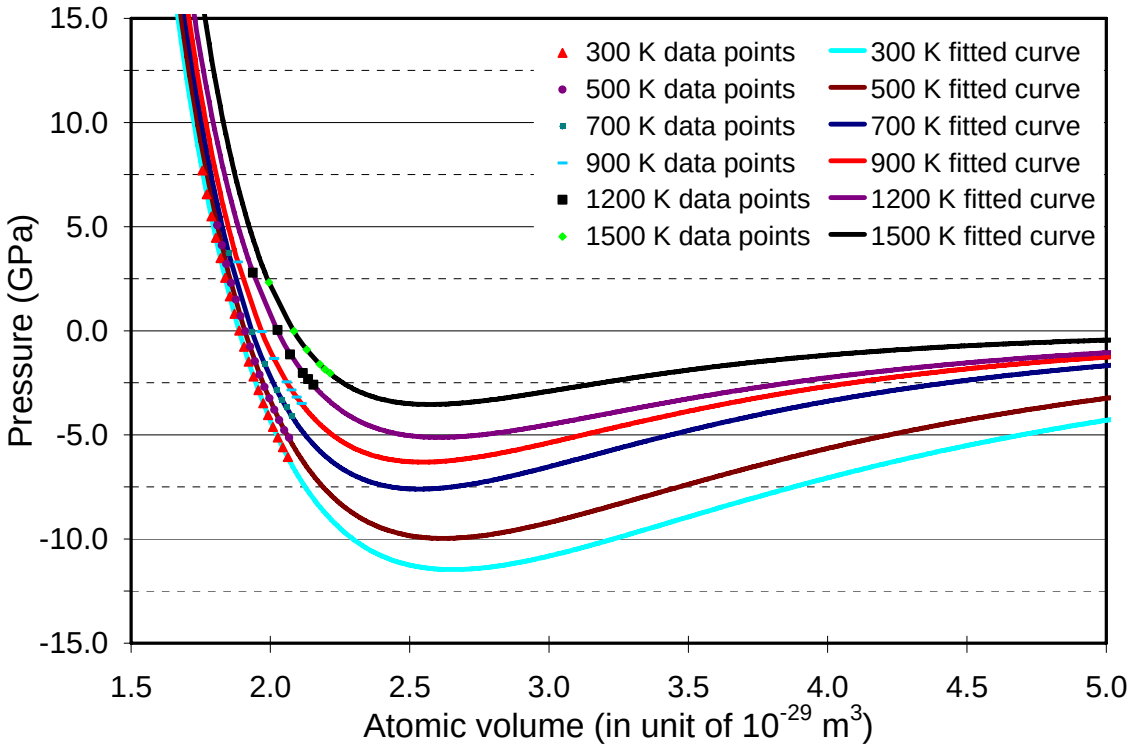

Figure 4.1. Pressure change with atomic volume at different temperatures of the $Cu_{46}Zr_{54}$ binary model metallic glass and liquid.

Cavitation phenomena have been previously studied in liquids like helium, both experimentally and through molecular simulations in Lennard-Jones liquids [19-25]. In this chapter, negative pressure is found to be critical for the cavitation nucleation to occur. The time history of pressure was treated as the primary indicator for the cavity formation and was recorded during the simulations at each density point. Fig. 4.2 shows the pressure evolution vs. time at 300 K with a beginning pressure of ~ -6.05 GPa and ~ -6.3 GPa, respectively. It's clearly seen from Fig. 4.2 (a) that the pressure fluctuates and equilibrates at a constant level of ~ 6.05 GPa through the whole simulation period of 100 ps, and therefore no cavity is formed. However, when the pressure approaches ~ -6.3 GPa, cavitation occurs after pressure fluctuates for ~ 5 ps. As shown in Fig. 4.2 (b), voids are not generated immediately with the pressure drop, and the pressure fluctuates out to ~ 5 ps. At this point, the local pressure drops below the critical value; cavitation is triggered, followed by a rapid pressure increase. The cavitation pressure here is taken as the threshold pressure that triggers the cavitation process simultaneously. A careful visual examination was done by checking the simulation cell to confirm cavity formation. After 100 ps of simulation, a cavity of ~ 1 nm in diameter was found in the sample. Naturally, samples with cavities were not included in the data used to obtain the isothermal EOS diagram in Fig. 4.1.

Isothermal EOS fitting curves in Fig. 4.1 display a Van-Der-Waals-type loop This permits an estimation of the spinodal instability points from the locations of P vs. V. The thermodynamic limit of metastability at a certain temperature is the point at which the pressure-volume diagram exhibits a minimum, termed the spinodal pressure. Kinetically, voids are formed at a pressure above the spinodal pressure (at a fixed temperature) owing

to the density fluctuations. We call this the cavitation pressure. Fig. 4.3 shows the cavitation pressure as well as the spinodal pressure vs. temperature. Interestingly, it is found that the cavitation nearly always occurs when the negative pressure approaches ~ 1/2 the value of the spinodal instability pressure.

To save the computational cost of simulations, we systematically studied the cavitation behavior of the Cu-Zr binary model liquids at T = 1200 K. The results support the fact that pressure is the key for controlling cavitation. Starting from the state point corresponding to a volume of $2.15*10^{-29}$ m^3 and a pressure of -2.58 GPa, we increased the simulation temperature to 1300 K while still fixing the volume. No cavitation was found even when the higher temperature stimulates faster kinetic movements of the atoms. However, when the simulation cell temperature was reduced to 1150 K, cavitation was triggered due to the more negative pressure. We carefully examined the cavitation kinetics. Here, the cavitation time is defined as the time interval from the starting point of the simulation to the time where cavitation nucleates. Figure 4.4 shows the pressure dependence of the cavitation time at T = 1200 K. The existence of an energy barrier for nucleation of a first-order phase transition such as cavitation is quite general. A common model usually used to study cavitation nucleation is the classical nucleation theory [20]. The energy barrier exists because the interface between the two phases (liquid and vapor) has a finite surface energy per unit area. This energy is the vapor/liquid surface tension α of the model liquid. Since α is nonzero, the formation of a void with radius R has an energy cost of $4\pi R^2\alpha$. When such a void forms, the energy of the whole system contains the work of the negative pressure *P* over the void volume, so that the total energy cost of forming the cavity is

$$\Delta E = 4\pi R^2 \alpha + \frac{4\pi}{3} R^3 P \,. \tag{4.4}$$

At negative pressures, this energy has a maximum for a critical radius, $R_c = 2\alpha/|P|$. The energy at this radius establishes the energy barrier for a cavity formation, which is

$$\Delta E = \frac{16\pi\alpha^3}{3P^2} \,. \tag{4.5}$$

A thermal fluctuation may enable the system to cross this energy barrier. The probability of such an occurrence is proportional to the factor

$$\exp(-\Delta E / kT) \,, \tag{4.6}$$

where T is the absolute temperature and k is Boltzmann's constant. In this simplified model, it is clear that cavitation should be a random process that depends on the temperature and pressure. Therefore, the rate of cavitation nucleation is determined by

$$J = \gamma_0 \exp(-16\pi\alpha^3 / 3P^2 kT) \,, \tag{4.7}$$

where γ_0 is the microscopic rate of the order of a longitudinal phonon, ~ 10^{13}. The fitting curve using the converse of this cavitation rate (the cavitation time scale) from classical nucleation theory is shown in Fig. 4.4 as the solid line. It agrees quite well with the simulation data. From the fitting parameters, we can estimate the number of atoms involved for cavitation nucleation. At a pressure of -2.52 GPa and 1200 K, a barrier height of ~ 4 eV is estimated and ~ 10 to 100 atoms should be involved in the activated configuration to overcome this energy barrier and to initiate the cavitation.

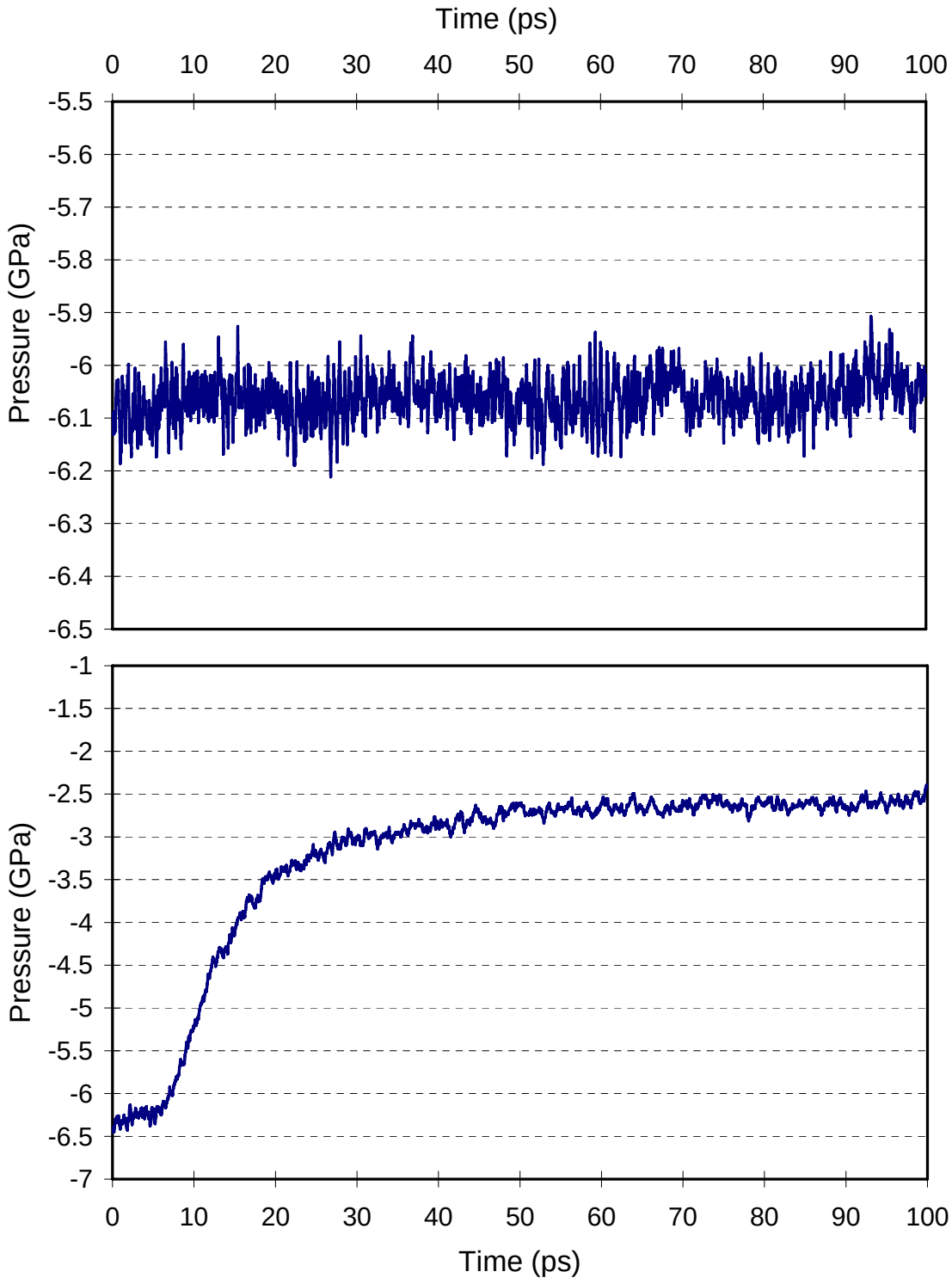

Figure 4.2. Pressure evolution vs. time at 300 K during the whole simulation process.

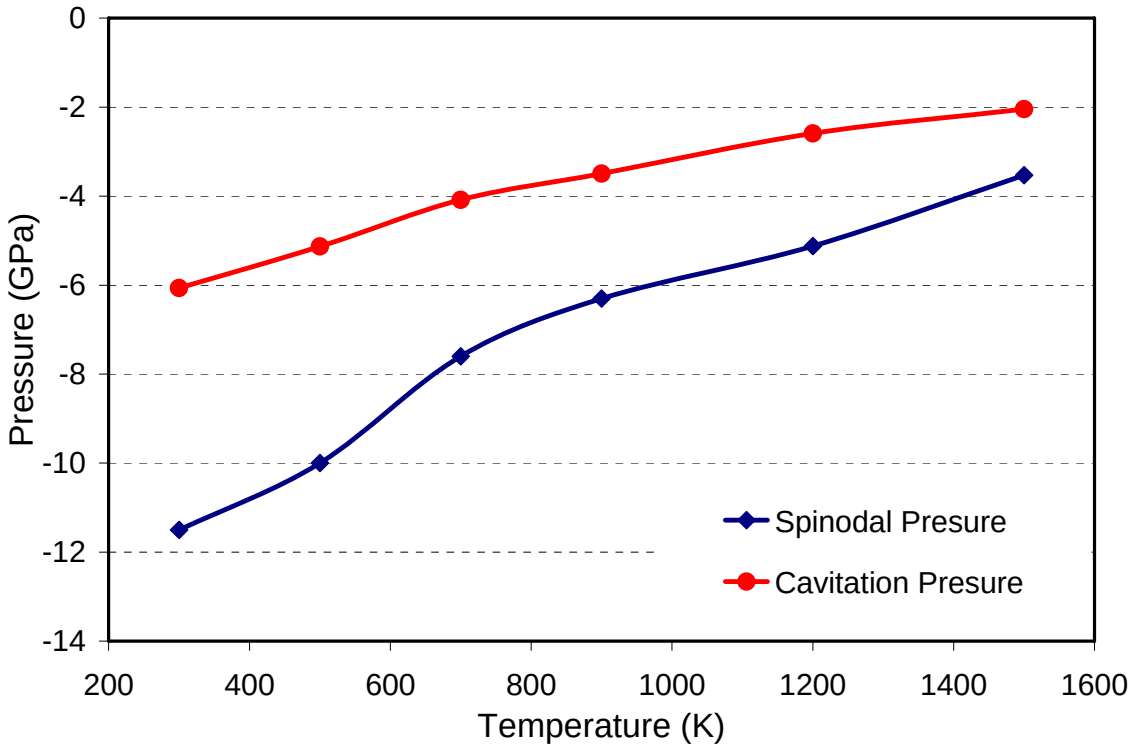

Figure 4.3. Cavitation pressure and spinodal pressure as a function of temperature.

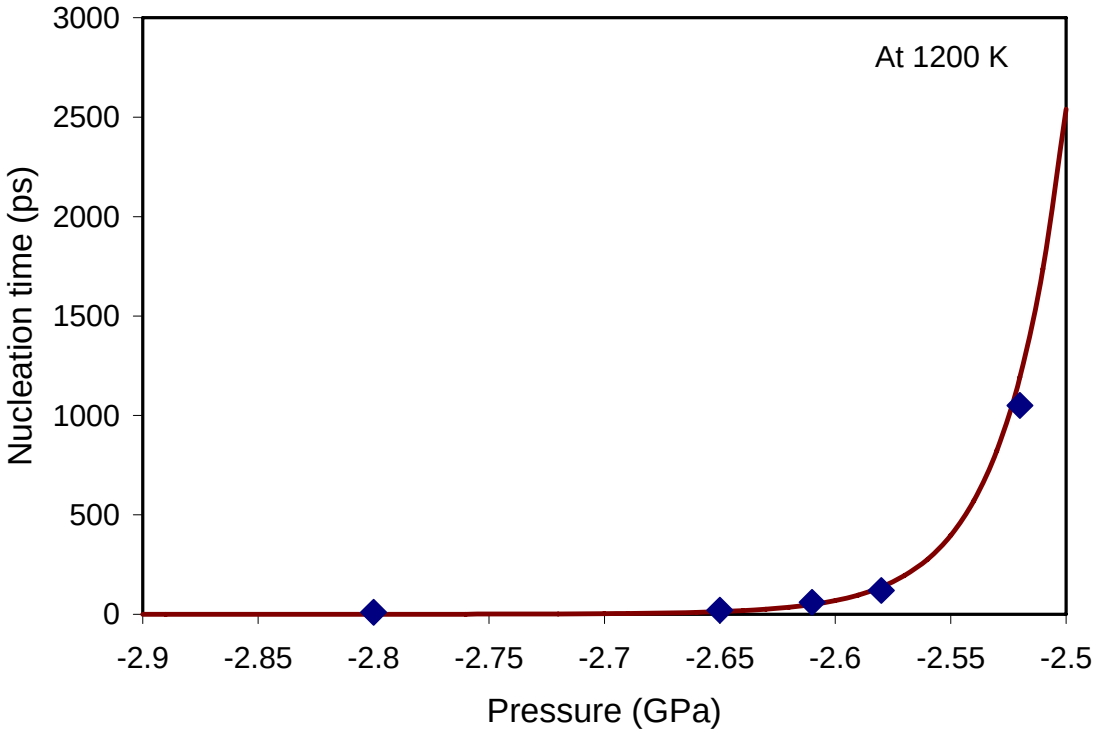

Figure 4.4. Cavitation time vs. pressure at T=1200 K and the fitting curve obtained from classical nucleation theory.

Considering the fact that the pressure is proportional to the equilibrium bulk modulus, $B_0(T)$ in the Vinet-Smith-Ferrante-Rose universal EOS, we notice that a higher spinodal pressure will be obtained for a material with higher B if the other two factors, X and $\eta_0(T)$ (see Equations 4.1-4.3) remain constants. This implies that it is more difficult for a void to form in the equilibrium system. One expects that B must be related to the barrier height for cavitation nucleation. Recall from the previous studies on the cooperative shear model, that the shear flow barrier in the glassy states is proportional to the isoconfigurational shear modulus G [9]. The barrier W for shear flow is related through a scaling law to a universal critical yield strain γ_{C0}, the shear modulus G for a fixed glass configuration, and the effective volume of cooperative shear zones (CSZ) $\Omega_{eff} = \zeta\Omega$.

$$W = \left(\frac{8}{\pi^2}\right) G\gamma_c^2 \zeta\Omega \tag{4.8}$$

The core volume of a CSZ is Ω and ζ is an "Eshelby" factor correcting for matrix confinement of the CSZ. From this model, a lower G value implies easier hopping between local energy minima in the potential energy landscape. Combining shear and cavitation events, we propose that the plasticity of metallic glasses is controlled by the number of shear events that occur before a catastrophic cavitation event is triggered. The ratio of G/B is then related to the ratio of the shear barrier to the cavitation barrier and therefore to the relative rate of cooperative shearing vs. cavitation events [26]. When a metallic glass is subjected to an applied load which includes negative hydrostatic pressure (e.g., uniaxial tension), the nucleation slip on a shear band would be limited by the nucleation of

cavitation within the shear band core. In turn, the total accumulated shear band slip proceeding cavitation would be related to the ratio of the barrier height of the two processes. This is then related to G/B and to Poisson's ratio. This approach may provide a rationale for the reported correlation between fracture toughness, ductility and G/B (or ν).

4.4. Chapter Concluding Remarks

In summary, we determined the isothermal equation of state (EOS) in a wide range of temperatures and pressures by carrying out molecular dynamics simulations on a simple binary model metallic glass. A universal form of EOS proposed by Vinet et al. was utilized to fit the data, assuming no phase transitions. Pressure-induced cavitation was observed in glassy states and liquids from our simulations. The thermodynamic limit of instability and kinetic limit of instability for cavitation behavior were analyzed. Negative pressure is a critical parameter in triggering cavitation. The cavitation barrier height was estimated from the classical nucleation theory. A possible explanation for the reported correlation between ductility, fracture toughness, G/B, and Poisson's ratio was suggested.

References

[1] W. L. Johnson, MRS Bulletin 24, 42 (1999).

[2] A. Inoue, Acta Materialia 48, 279 (2000).

[3] W. H. Wang, C. Dong, and C. H. Shek, Materials Science & Engineering R-Reports 44, 45 (2004).

[4] W. H. Wang, Z. X. Bao, C. X. Liu, et al., Physical Review B 61, 3166 (2000).

[5] W. H. Wang, P. Wen, L. M. Wang, et al., Applied Physics Letters 79, 3947 (2001).

[6] P. Vinet, J. R. Smith, J. Ferrante, et al., Physical Review B 35, 1945 (1987).

[7] P. G. Debenedetti and F. H. Stillinger, Nature 410, 259 (2001).

[8] D. J. Lacks, Physical Review Letters 8722, 225502 (2001).

[9] W. L. Johnson and K. Samwer, Physical Review Letters 95 195501 (2005).

[10] M. L. Lind, G. Duan, and W. L. Johnson, Physical Review Letters 97 015501 (2006).

[11] G. Duan, M. L. Lind, M. D. Demetriou, et al., Applied Physics Letters 89 151901(2006).

[12] M. D. Demetriou, J. S. Harmon, M. Tao, et al., Physical Review Letters 97 065502 (2006).

[13] V. N. Novikov and A. P. Sokolov, Nature 431, 961 (2004).

[14] V. N. Novikov and A. P. Sokolov, Physical Review B 74 064203 (2006).

[15] G. Duan, M. L. Lind, K. De Blauwe, et al., Applied Physics Letters 90 211901 (2007).

[16] Z. F. Zhang, J. Eckert, and L. Schultz, Acta Materialia 51, 1167 (2003).

[17] Q. K. Li and M. Li, Physical Review B 75 094101 (2007).

[18] G. Duan, D. H. Xu, Q. Zhang, et al., Physical Review B 71 224208 (2005).

[19] C. Y. W. Wu, Nanoscale and Microscale Thermophysical Engineering 7, 137 (2003).

[20] H. Maris and S. Balibar, Physics Today 53, 29 (2000).

[21] D. S. Corti and P. G. Debenedetti, Chemical Engineering Science 49, 2717 (1994).

[22] D. S. Corti, P. G. Debenedetti, S. Sastry, et al., Physical Review E 55, 5522 (1997).

[23] V. K. Shen and P. G. Debenedetti, Journal of Chemical Physics 111, 3581 (1999).

[24] V. K. Shen and P. G. Debenedetti, Journal of Chemical Physics 114, 4149 (2001).

[25] V. K. Shen and P. G. Debenedetti, Journal of Chemical Physics 118, 768 (2003).

[26] J. J. Lewandowski, W. H. Wang, and A. L. Greer, Philosophical Magazine Letters 85, 77 (2005).